Int. J. Solids Structures Vol. 31, No. 1, pp. 51–64, 1994
Printed in Great Britain

0020–7683/94 $6.00+.00

SURFACE CRACKS IN TRANSFORMATION TOUGHENING CERAMICS

J. H. ANDREASEN
Institut for Maskinteknik, Aalborg University, Denmark

and

B. L. KARIHALOO
School of Civil and Mining Engineering, University of Sydney, Australia

(*Received* 1 *February* 1993; *in revised form* 22 *July* 1993)

Abstract—This paper presents a complete R-curve analysis for a single surface crack and an array of equally spaced parallel surface cracks in transformation toughened ceramics (TTC). The problem is reduced to the solution of a pair of singular integral equations in which the dislocation density function and the transformation zone boundary are the unknown functions. The form of the equations does not depend on the number of surface cracks being studied; only the weight functions are different. The singularities of the weight functions and of the dislocation density functions at the crack tip and at the intersection of the crack by the transformation zone wake are analytically isolated for accurate numerical integration of the integral equations.

1. INTRODUCTION

High stresses such as exist at sharp crack tips induce tetragonal to monoclinic phase transformation in zirconia ceramics as a result of which these ceramics have a higher fracture toughness. The mechanics of transformation toughened ceramics has been extensively studied by many researchers in the past decade [e.g. McMeeking and Evans (1982); Budiansky *et al.* (1983); Rose (1987)]. Earlier studies concentrated on the steady-state toughening configuration, wherein a semi-infinite planar crack was surrounded by a semi-infinite zone of transformed material. Subsequently, a complete R-curve analysis of the growing crack was performed from the onset of its growth to the attainment of steady-state conditions, both for a semi-infinite crack (Stump and Budiansky, 1989a) and a finite internal crack (Stump and Budiansky, 1989b; Andreasen, 1990; see also Andreasen and Karihaloo, 1992). A recent paper by Stump (1992) solved the problem of a single surface crack growing in a material containing a pre-existing transformation zone, thus avoiding many mathematical difficulties (see later).

This paper presents a complete R-curve analysis of a single surface crack and an array of equally spaced parallel surface cracks in transformation toughened ceramics. These surface crack models are expected to be a good approximation for surface damage and therefore a good basis for analysing the thermal shock, thermal fatigue, wear and other phenomena in transformation toughened ceramics. The problem of surface cracks in non-transforming elastic materials has been solved by many investigators. The works of Nemat-Nasser *et al.* (1978), Keer *et al.* (1979), and Nemat-Nasser *et al.* (1980) which address the stability of surface cracks are of particular interest to this paper.

The configuration of an array of equally spaced (spacing d) parallel surface cracks in a transformation toughened ceramic is depicted in Fig. 1. A single surface crack can be thought of as a special case of this configuration in which $d \to \infty$. However, in the analysis to follow, the single surface crack geometry is studied first and then generalised to an array of surface cracks. The length of each crack in the array is c, and the half plane is assumed to be loaded at infinity by a constant stress σ^{∞} normal to the cracks. As the external stress is applied a zone of transformed material S forms at each crack tip. It is assumed that the tetragonal to monoclinic transformation is induced when the mean stress attains a critical value σ_m^c. In common with most previous investigations, it is assumed that the trans-

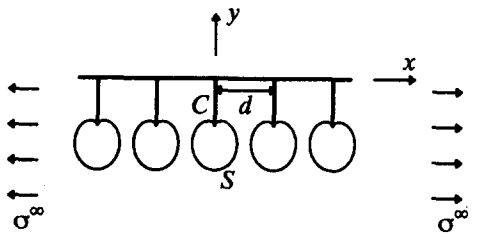

Fig. 1. Model configuration for an array of parallel surface cracks.

formation strains are purely dilatational and constant inside the zone S. The effects of elastic mismatch between the transformed and non-transformed particles (Huang *et al.*, 1993) and variability of dilatational strain inside the zone (Karihaloo, 1991) are ignored, and no reverse transformation is assumed to take place.

2. MATHEMATICAL FORMULATION

Each crack in the array is modelled by a pile-up of dislocations (Fig. 2). First, the free surface problem is solved analytically for a dislocation using Muskhelishvili's theory of plane elasticity. Then the density of dislocations in the pile-up is adjusted to meet the traction free condition on the crack faces. The transformation zone boundary ahead of each crack tip is determined by the critical mean stress criterion, but first the free surface problem for a homogeneous inclusion of arbitrary shape is solved by using Eshelby formalism and Muskhelishvili's theory of plane elasticity. Finally, the dislocation density function and the transformation zone boundary are determined from the solution of two coupled singular integral equations.

We recapitulate first the essential steps in the derivation of the governing equations for the elastic problem of an arbitrarily placed single surface crack with its transformation zone (Fig. 3). The governing equations are stated in terms of certain weight functions. For

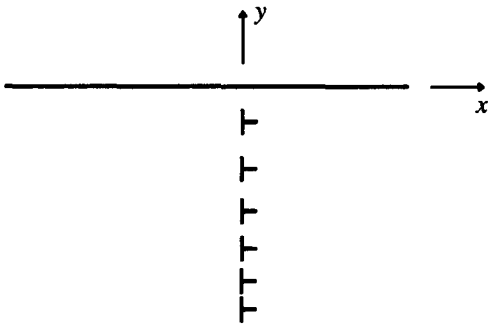

Fig. 2. Dislocation pile up for modelling a single surface crack.

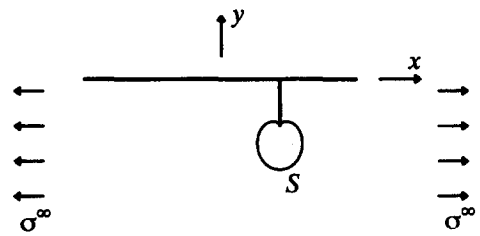

Fig. 3. Model configuration for an arbitrarily placed surface crack.

the description of an array of equally spaced parallel surface cracks the governing equations retain the same form; only the weight functions are different.

The complex potentials for a dislocation with Burgers vector in the x-direction and located at $z_0 = x_0 + iy_0$ under plane strain conditions (Fig. 3) were given by Muskhelishvili:

$$\Phi_\infty^D(z) = \frac{-ibE}{8\pi(1-\nu^2)(z-z_0)}$$

$$\Psi_\infty^D(z) = \frac{ibE}{8\pi(1-\nu^2)}\left(\frac{1}{(z-z_0)} - \frac{\bar{z}_0}{(z-z_0)^2}\right), \tag{1}$$

where E is Young's modulus, ν is Poisson's ratio and b is the magnitude of Burgers vector.

The complex potentials for a homogeneous inclusion with uniform dilatational strains ε^T can be obtained in several ways. One can use the concept of centres of strains (Rose, 1987) or one can use the Eshelby formalism together with Muskhelishvili's theory of plane elasticity. Whichever route one takes, the potentials are:

$$\Phi_\infty^T(z) = A$$

$$\Psi_\infty^T(z) = \frac{E\varepsilon^T}{2\pi(1-\nu)}\left(\int_S \frac{i}{z-z_0}\,\mathrm{d}x_0 + B\right), \tag{2}$$

where $A = -[E\varepsilon^T]/[4(1-\nu)]$, $B = -\pi$ for $z \in S$, and $A = B = 0$, otherwise.

In (1) and (2) and the sequel, superscripts D and T refer to dislocations and transformation, respectively. The stresses corresponding to the complex potentials of (1) and (2) are calculated from:

$$\sigma_{xx}^\infty + \sigma_{yy}^\infty = 2\{\Phi_\infty + \overline{\Phi_\infty(z)}\}$$

$$\sigma_{yy}^\infty - \sigma_{xx}^\infty + 2i\sigma_{xy}^\infty = 2\{\bar{z}\Phi'_\infty(z) + \Psi_\infty(z)\}, \tag{3}$$

where Φ_∞ can be Φ_∞^D or Φ_∞^T, and similarly for Ψ_∞, an overbar denotes complex conjugate and a prime differentiation with respect to z.

In order to annul the stresses on the free surface $y = 0$, it is necessary to modify the above full plane potentials. However, half plane problems can be solved using just one potential. Muskhelishvili has shown how to construct a potential Φ_0 for a half plane with prescribed stresses σ_{yy} and σ_{xy} on the free surface $y = 0$,

$$\Phi_0(z) = -\frac{1}{2\pi i}\int_{-\infty}^{\infty} \frac{\sigma_{yy} - i\sigma_{xy}}{t-z}\,\mathrm{d}t. \tag{4}$$

The half plane potential $\Phi_0^D(z)$ for a dislocation is obtained from (4) with $\sigma_{yy} - i\sigma_{xy} = -(\sigma_{yy}^\infty - i\sigma_{xy}^\infty)$, where $\sigma_{yy}^\infty - i\sigma_{xy}^\infty$ are the stresses corresponding to (1) at $y = 0$,

$$\Phi_0^D(z) = \begin{cases} \dfrac{iEb}{8\pi(1-\nu^2)}\dfrac{z-z_0}{(z-\bar{z}_0)^2}; & y < 0 \\ -\dfrac{iEb}{8\pi(1-\nu^2)}\dfrac{1}{z-z_0}; & y > 0. \end{cases} \tag{5}$$

The half plane potential $\Phi_0^T(z)$ for the transformation zone is similarly determined from (2)–(4) to be:

$$\Phi_0^T(z) = \frac{E\varepsilon^T}{2\pi(1-\nu)} \int_S \frac{i}{z-\bar{z}_0}\,\mathrm{d}x_0\,; \quad y<0 \tag{6}$$

$\Phi_0^T(z) = 0$ when $y > 0$. The stresses corresponding to the half-plane potentials are determined from:

$$\begin{aligned} \sigma_{xx}^0+\sigma_{yy}^0 &= 2\{\Phi_0(z)+\bar{\Phi}_0(\bar{z})\} \\ \sigma_{yy}^0-\sigma_{xx}^0+2i\sigma_{xy}^0 &= 2\{(\bar{z}-z)\Phi_0'(z)-\Phi_0(z)-\bar{\Phi}_0(z)\}. \end{aligned} \tag{7}$$

The total stress σ_{xx}^c across the crack must vanish. This stress is made up of the externally applied field and contributions from the pile-up of dislocations representing the crack and from the transformation zone. The former contribution can be written as:

$$\int_C \sigma_{xx}^D(z, z_0)D(y_0)\,\mathrm{d}y_0/b,$$

where $D(y_0)$ is the dislocation density function such that $D(y_0)\,\mathrm{d}y_0$ is the Burgers vector of the dislocations between y_0 and $y_0+\mathrm{d}y_0$, and the latter $\sigma_{xx}^T(z)$.

The stress σ_{xx}^D due to a single dislocation is calculated from (1), (3), (4), (5) and (7) and the stress σ_{xx}^T from (2), (3), (4), (6) and (7). Introducing the weight functions $g^D(\underline{z}, \underline{z}_0)$ and $g^T(\underline{z}, \underline{z}_0)$, the traction free condition along the crack can be written as:

$$0 = \left(\sigma^\infty + \frac{E\varepsilon^T}{2\pi(1-\nu)}\int_S g^T(\underline{z}, \underline{z}_0)\,\mathrm{d}x_0 + \frac{E}{4\pi(1-\nu^2)}\int_C D(y_0)g^D(\underline{z}, \underline{z}_0)\,\mathrm{d}y_0\right)_{z\in C}. \tag{8}$$

The underscored arguments indicate functional dependence on the Cartesian coordinates x and y. For an arbitrarily placed single surface crack the real weight functions $g^D(\underline{z}, \underline{z}_0)$ and $g^T(\underline{z}, \underline{z}_0)$ are:

$$g^T(\underline{z}, \underline{z}_0) = \frac{3(y+y_0)}{(y+y_0)^2+(x-x_0)^2} - 2y\frac{(y+y_0)^2-(x-x_0)^2}{[(y+y_0)^2+(x-x_0)^2]^2} - \frac{(y-y_0)}{(y-y_0)^2+(x-x_0)^2}, \tag{9}$$

$$\begin{aligned} g^D(\underline{z}, \underline{z}_0) = {} & \frac{2(y+y_0)}{(y+y_0)^2+(x-x_0)^2} - (y+3y_0)\frac{(y+y_0)^2-(x-x_0)^2}{[(y+y_0)^2+(x-x_0)^2]^2} \\ & + 4yy_0(y+y_0)\frac{(y+y_0)^2-3(x-x_0)^2}{[(y+y_0)^2+(x-x_0)^2]^3} - (y-y_0)\frac{(y-y_0)^2+3(x-x_0)^2}{[(y-y_0)^2+(x-x_0)^2]^2}. \end{aligned} \tag{10}$$

The integral eqn (8) in the unknown density function $D(y_0)$ applies for any arbitrarily placed surface crack. By summing the stresses from each crack and its corresponding transformation zone in the self-similar array of equally spaced surface cracks two new weight functions, denoted $G^D(\underline{z}, \underline{z}_0)$ and $G^T(\underline{z}, \underline{z}_0)$, are obtained from $g^D(\underline{z}, \underline{z}_0)$ and $g^T(\underline{z}, \underline{z}_0)$. Substituting these into the integral eqn (8) gives the zero traction condition across each crack in the array. Details of $G^D(\underline{z}, \underline{z}_0)$ and $G^T(\underline{z}, \underline{z}_0)$ are given in the Appendix.

In order to determine the transformation zone boundary S we use the critical mean stress criterion for transformation. The mean stress in the plane strain conditions is given by:

$$\sigma_m = \frac{1+\nu}{3}(\sigma_{xx}+\sigma_{yy}) = \tfrac{4}{3}(1+\nu)\Re\{\Phi(z)\}. \tag{11}$$

Equation (11) holds for both plane and half-plane potentials. Superposition of the stresses from the applied field, dislocations and transformation, using (11), gives:

$$\sigma_m^c = \frac{1+\nu}{3}\left(\sigma^\infty + [\sigma_{xx}^T(z)+\sigma_{yy}^T(z)] + \int_C [\sigma_{xx}^D(z,z_0)+\sigma_{yy}^D(z,z_0)]\frac{D(y_0)}{b}\,dy_0\right)_{z\in S}. \tag{12}$$

Finally, from (1), (2), (3), and (5)–(7) and (12) one obtains the following integral equation for the determination of the transformation zone boundary:

$$1 = \frac{1+\nu}{3\sigma_m^c}\left(\sigma^\infty + \frac{E\varepsilon^T}{2\pi(1-\nu)}\int_S h^T(\underline{z},\underline{z}_0)\,dx_0 + \frac{E}{4\pi(1-\nu^2)}\int_C D(y_0)h^D(\underline{z},\underline{z}_0)\,dy_0\right)_{z\in S}. \tag{13}$$

The weight functions $h^D(\underline{z},\underline{z}_0)$ and $h^T(\underline{z},\underline{z}_0)$ in (13) are given by:

$$h^T(\underline{z},\underline{z}_0) = \frac{4(y+y_0)}{(y+y_0)^2+(x-x_0)^2} \tag{14}$$

$$h^D(\underline{z},\underline{z}_0) = \frac{2(y+y_0)}{(y+y_0)^2+(x-x_0)^2} - 4y_0\frac{(y+y_0)^2-(x-x_0)^2}{[(y+y_0)^2+(x-x_0)^2]^2} - \frac{2(y-y_0)}{(y-y_0)^2+(x-x_0)^2}. \tag{15}$$

As before, two new weight functions $H^D(\underline{z},\underline{z}_0)$ and $H^T(\underline{z},\underline{z}_0)$ can be obtained from (14) and (15) by summing the mean stresses from each crack in the self-similar array of equally spaced parallel cracks. Substitution of these weight functions into (13) gives the integral equation for the determination of the transformation zone boundary S of each crack in the array. Details of $H^D(\underline{z},\underline{z}_0)$ and $H^T(\underline{z},\underline{z}_0)$ are given in the Appendix.

This concludes the derivation of the governing equations for the elastic problem depicted in Fig. 1.

3. NUMERICAL SOLUTION

It is convenient to rewrite (8) and (13) in a form suitable for analysing the R-curve behaviour of TTC. To do this, we use the measure of transformation strength ω, introduced by Amazigo and Budiansky (1988) and the length measure L of Stump and Budiansky (1989a):

$$\omega = \frac{Ec_p\theta_p^T}{\sigma_m^c}\left(\frac{1+\nu}{1-\nu}\right); \quad L = \frac{2}{9\pi}\left(\frac{K^c(1+\nu)}{\sigma_m^c}\right)^2, \tag{16}$$

where K^c is the intrinsic fracture toughness of the ceramic, θ_p is the dilatation caused by the transformation of a particle and c_p is the fraction of transformed particles in the composite TTC. Moreover, the far-field mode I stress state σ^∞ is expressed through an applied stress intensity factor:

$$\sigma^\infty = \frac{K^{\text{app}}}{B_0\sqrt{\pi c}}, \tag{17}$$

where the constant B_0 is approximately equal to 1.1215 for a single surface crack. For an

array of equally spaced parallel surface cracks, B_0 varies with the spacing d (see e.g. Murakami, 1987). Finally, we define a new dislocation density function $D^*(y_0)$ via:

$$D^*(y_0) = \frac{E}{12\pi\sigma_m^c(1-\nu)} D(y_0). \tag{18}$$

Substitution of (16)–(18) into the integral equations (8) and (13) gives:

$$0 = \frac{K^{app}}{B_0 K^c}\sqrt{\frac{L}{2c}} + \frac{\omega}{18\pi}\int_S g^T(\underline{z}, \underline{z}_0)\,dx_0 + \int_C D^*(y_0) g^D(\underline{z}, \underline{z}_0)\,d(y_0); \quad z \in C, \tag{19}$$

$$1 = \frac{K^{app}}{B_0 K^c}\sqrt{\frac{L}{2c}} + \frac{\omega}{18\pi}\int_S h^T(\underline{z}, \underline{z}_0)\,dx_0 + \int_C D^*(y_0) h^D(\underline{z}, \underline{z}_0)\,d(y_0); \quad z \in S. \tag{20}$$

Equations (19) and (20) determine the dislocation density function $D^*(y_0)$ and the transformation zone boundary S for a given remote load K^{app} and transformation strength ω for a single surface crack. The same equations also describe the array of parallel surface cracks when the weight functions g^T, g^D, h^T and h^D are replaced by G^T, G^D, H^T and H^D, respectively.

In order to analyse the initial toughening and subsequent R-curve behaviour it is necessary to impose a dynamic condition for crack growth. It is assumed that crack growth will begin and then continue in a quasi-static manner if the stress intensity factor at the crack tip K^{tip} equals the intrinsic fracture toughness of the ceramic:

$$K^{tip} = K^c \tag{21}$$

where, by definition:

$$\frac{K^{tip}}{K^c} = \lim_{y \to -c^-} 2\pi D^*(y)\sqrt{\frac{|c+y|}{L}}. \tag{22}$$

Combining (19)–(22) gives the following system of equations at the onset of crack growth:

$$0 = \frac{K^{app}}{B_0 K^c}\sqrt{\frac{L}{2c}} + \frac{\omega}{18\pi}\int_S g^T(\underline{z}, \underline{z}_0)\,dx_0 + \int_C D^*(y_0) g^D(\underline{z}, \underline{z}_0)\,d(y_0); \quad z \in C$$

$$1 = \frac{K^{app}}{B_0 K^c}\sqrt{\frac{L}{2c}} + \frac{\omega}{18\pi}\int_S h^T(\underline{z}, \underline{z}_0)\,dx_0 + \int_C D^*(y_0) h^D(\underline{z}, \underline{z}_0)\,d(y_0); \quad z \in S$$

$$1 = \lim_{y \to -c^-} 2\pi D^*(y)\sqrt{\frac{|c+y|}{L}}. \tag{23}$$

The unknowns in (23) are the applied stress intensity factor K^{app} that reflects the apparent fracture toughness at the onset of crack growth, the transformation zone boundary S and the dislocation density function $D^*(y_0)$.

The integral equations (23) contain a number of singularities. First, the dislocation density function $D^*(y_0)$ has the usual square root singularity at the crack tip (22). Secondly, as the crack line stress imposed by the transformation zone suffers a discontinuity when its wake crosses the crack, the dislocation density function has a logarithmic singularity. Thirdly, the weight functions contain singularities of the ordinary Cauchy type, as well as weak singularities at the surface ($y = 0$) and at the intersection of the crack by the transformation zone boundary. For accurate numerical solution of (23) it is imperative to

have good control over these singularities. This has been ensured by isolating the singularities and treating them analytically as far as possible, so that only smooth, non-singular functions are subject to numerical treatment. Details will be published elsewhere.

For a quasi-statically growing crack (23) have to be restated in an incremental form as follows:

$$0 = \frac{K^{app}}{B_0 K^c}\sqrt{\frac{L}{2c}} + \frac{\omega}{18\pi}\int_S g^T(\underline{z}, \underline{z}_0)\,dx_0 + \int_C D^*(y_0) g^D(\underline{z}, \underline{z}_0)\,d(y_0); \quad z \in C$$

$$1 = \frac{K^{app}}{B_0 K^c}\sqrt{\frac{L}{2c}} + \frac{\omega}{18\pi}\int_S h^T(\underline{z}, \underline{z}_0)\,dx_0 + \int_C D^*(y0) h^D(\underline{z}, \underline{z}_0)\,d(y_0); \quad z \in S_{front}$$

$$1 = \lim_{y \to -(c+\Delta c)^-} 2\pi D^*(y)\sqrt{\frac{|c+\Delta c+y|}{L}} \tag{24}$$

$S(c)_{wake} = S(c+\Delta c)_{wake}$.

The quasi-static growth regime has to be distinguished from the onset of crack growth because the iterative method of solution used for the determination of the transformation zone shape S assumes that the location at which the crack is crossed by the wake of the zone is prescribed and fixed during an iteration.

The solution of the system of eqns (23) was obtained by improving a starting guess for the transformation zone shape through a number of perturbations. By inverting the first integral equation (23) for each perturbed shape, an improved zone shape was obtained by Newton–Raphson method.

For the quasi-statically growing crack the last equation (24) expresses the fact that no reverse transformation is permitted. The transformation zone shape is only changed at the front S_{front} where the mean stress is rising, while a wake of transformed material is allowed to develop behind the tip of the growing crack where the mean stress is falling. The iterative procedure for the solution of (24) involved making a guess for the transformation zone front S_{front} and solving the first integral equation for the dislocation density function $D^*(y_0)$. Substitution of this result into the second integral equation permitted an improvement to be made on the assumed transformation zone shape. This iterative process was repeated until covergence was attained. The last two side conditions (24) were met by adjusting K^{app} iteratively and by joining the transformation zone wake S_{wake} and front S_{front} by common tangents.

4. RESULTS AND DISCUSSION

The presentation of results and discussion begins with an isolated surface crack and is followed by an array of surface cracks.

Figure 4 shows examples of transformation zone shapes at the onset of crack growth obtained by solving the set of eqns (23). A monotonic increase in transformation zone size

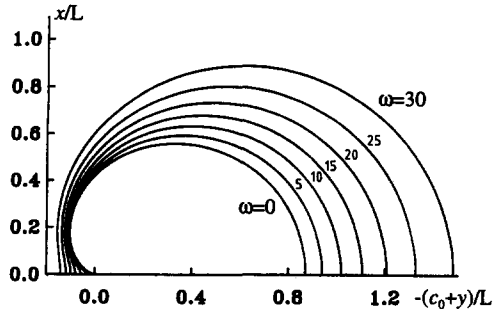

Fig. 4. Initial transformation zone shapes for a single surface crack. $c_0/L = 10$, $\omega = 0, 5, \ldots, 30$.

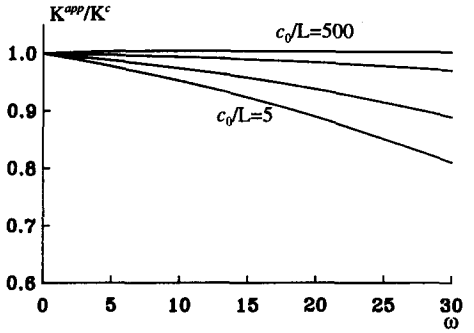

Fig. 5. SIFs at the onset of crack growth for single surface cracks. $c_0/L = 5, 10, 50, 500$.

with increasing ω is valid for initial crack lengths which are not too small. The critical initial crack length c_0 at which transformation zone diverges for vanishing ω corresponds to σ^∞ exceeding the critical mean stress σ_m^c before crack growth is initiated and is approximately equal to $c_0/L = 0.3975$ for a single surface crack. As for internal cracks an initial toughness decrement appears for these critical cracks and consequently the transformation zone size becomes bounded for nonzero values of the transformation parameter ω even for an initial crack length equal to the critical crack length. It is a characteristic of the present model that the transformation zone detaches from the crack tip for $\omega > 0$.

The apparent toughness at the onset of crack growth for several initial crack lengths is shown in Fig. 5. A toughness decrement is observed before crack growth is induced. For longer initial crack lengths however a slight toughness increment is observed. The toughening for a semi-infinite crack is within 0.5% of the toughening for the surface crack with initial length $c_o/L = 500$. The trend of decreasing toughness for shorter initial cracks is in agreement with the results for internal cracks (Stump and Budiansky, 1989a).

Figures 6 and 7 show the R-curves determined from equations (24) for several initial crack lengths and for values of the transformation density ω equal to 5 and 10, respectively.

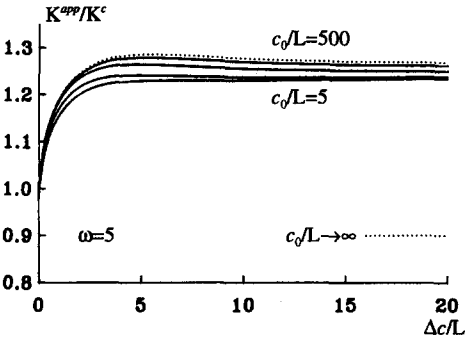

Fig. 6. R-curves for single surface cracks. $c_0/L = 5, 10, 50, 500$.

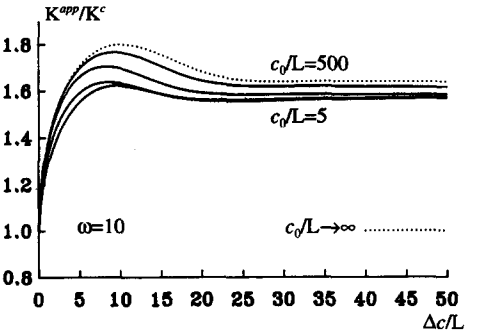

Fig. 7. R-curves for single surface cracks. $c_0/L = 5, 10, 50, 500$.

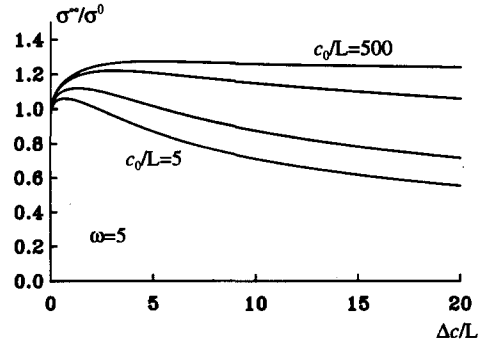

Fig. 8. Applied stress for single surface cracks. $c_0/L = 5, 10, 50, 500$.

The limiting cases of infinite initial crack lengths were first obtained by Stump and Budiansky (1989a). Peaks in toughening appear before steady-state conditions are reached. The presence of the free surface causes these peaks to get shallower with decreasing initial crack length; the peaks may even be less than the steady-state toughness, as seen for an initial crack length $c_0/L = 5$ in Fig. 7. Monotonically rising R-curves can be seen most vividly for $c_0/L = 5$ in Fig. 6, but such behaviour is the exception rather than the rule for surface cracks. It is worth noting that the results of Figs 6 and 7 compare very favourably with Stump's results (1992). To see this, one need just compare these figures with the solid lines in Fig. 9 of Stump's paper. Of course, the toughening ratios at the onset of crack extension will be different because Stump considers growth from a pre-existing transformation zone.

The appearance of peaks in toughening prior to the attainment of steady-state toughening seems to be an inherent feature of models based on the critical mean stress transformation criterion, and are found for semi-infinite cracks (Stump and Budiansky, 1989a), for uniaxially loaded internal cracks (Stump and Budiansky, 1989b), for biaxially loaded internal cracks (Andreasen, 1990), and for shorter initial crack lengths. The results for a surface crack are similar to those for uniaxially loaded internal cracks (Stump and Budiansky, 1989b), but contrast with the results for internal cracks under equal biaxial loading (Andreasen, 1990). The results for infinite initial crack lengths shown by broken curves in Figs 6 and 7 have converged to within a fraction of a percent of the steady-state toughening value (Amazigo and Budiansky, 1988). In comparison with semi-infinite cracks the convergence to steady-state conditions by the R-curves for finite initial crack lengths was considerably slower.

The applied stress at infinity σ^∞ necessary for maintaining quasi-static crack growth is shown in Figs 8 and 9 for several initial crack lengths and for values of the transformation parameter ω equal to 5 and 10 corresponding to the R-curves of Figs 6 and 7, respectively. The applied stress is obtained from the following relation between stress and toughness:

$$\frac{\sigma^\infty(\Delta c)}{\sigma^0} = \frac{K^{\text{app}}(\Delta c)}{K^c}\sqrt{\frac{c_0}{c_0+\Delta c}}, \tag{25}$$

where the normalizing stress σ^0 is the stress necessary to induce crack growth in the absence of transformation.

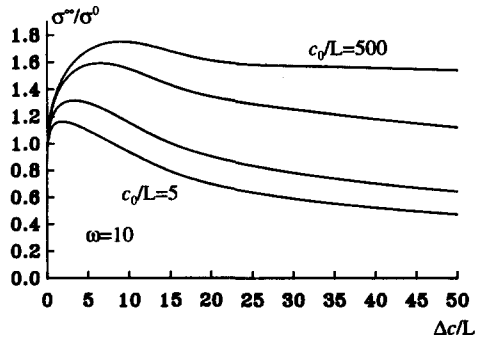

Fig. 9. Applied stress for single surface cracks. $c_0/L = 5, 10, 50, 500$.

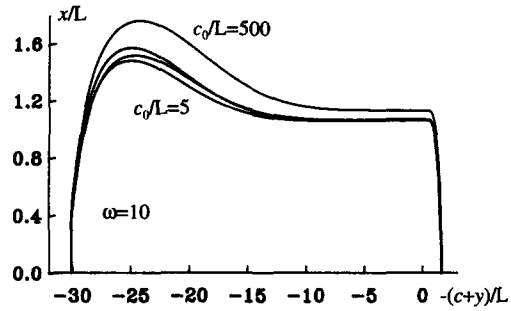

Fig. 10. Transformation zone shapes for single surface cracks. $c_0/L = 5, 10, 50, 500, \Delta c/L = 30$.

A comparison of R-curves with the corresponding curves for the applied stress reveals that the peaks in the stress, determining the ultimate strength, appear at distances of crack growth which are shorter than those necessary for peak toughness. Thus the peak toughness is not fully available for the strengthening of the material except for very long initial crack lengths.

The peaks in the R-curve behaviour result from the widening of transformation zone as seen in Fig. 10. As with the peaks in toughening, the zone widening diminishes with decreasing initial crack length.

Reciprocal peak toughening is shown in Fig. 11 for values of the transformation parameter ω up to 16. Lock-up values of this parameter at which divergence of the transformation zone appears and the toughness peak tends to infinity have not been determined. For initial crack lengths of $c_0/L = 5$ and 10 the lock-up values are less than the lock-up value of $\omega = 20.2$ for semi-infinite cracks (Stump and Budiansky, 1989a), whereas the lock-up for initial crack lengths of $c_0/L = 50$ and 500 is expected to appear at values intermediate between the lock-up value for semi-infinite cracks and for steady-state conditions ($\omega = 30.0$). The peak toughening is the smaller the shorter the initial crack length for values of transformation parameter which is not too high. For ω larger than about 12 a change in this trend is noticed as the peak toughness for shorter cracks exceeds that for longer cracks.

Reciprocal peak strengthening is shown in Fig. 12 for values of the transformation parameter up to 20. The results are consistent with the results for internal cracks in that initially weak materials with long inherent cracks are more susceptible to strengthening than initially strong materials.

The decrease in strengthening appearing for increasing values of the transformation parameter for the shorter initial crack lengths is due to softening of the R-curve, i.e. the slope of the R-curve diminishes for short crack growth distances. For $\omega = 20$ divergence of the transformation zone appears for initial crack lengths of $c_0/L = 5$ and 10 for finite crack growth distances, thus the lock-up value for ω has been exceeded.

We now present some results for arrays of surface cracks. The influence of interaction of the cracks in the array is emphasized by comparing the results with a single surface crack.

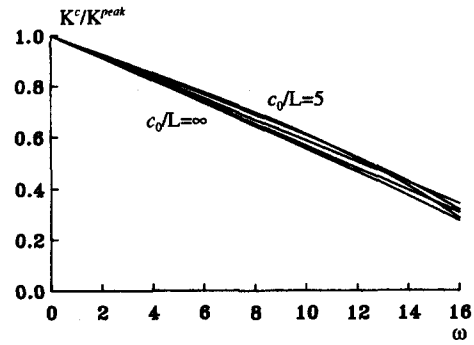

Fig. 11. Reciprocal peak toughening. $c_0/L = 5, 10, 50, 500, \infty$.

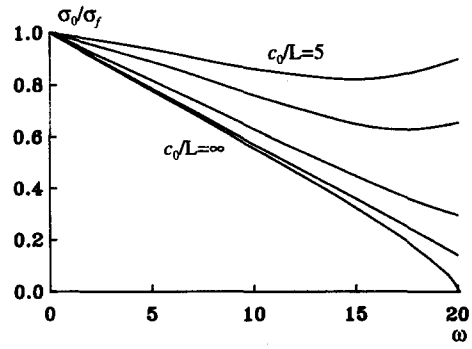

Fig. 12. Reciprocal peak strengthening. c_0/L = 5, 10, 50, 500, ∞.

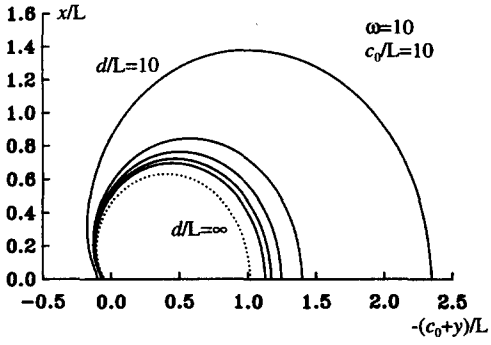

Fig. 13. Initial transformation zone shapes for an array for surface cracks. d/L = 10, 20, 30, 40, 50, ∞.

Examples of initial transformation zone shapes for an array of surface cracks obtained by solving eqns (23) with the weight functions given in the Appendix, are shown in Fig. 13 for several crack spacings. The initial toughening accompanying the zones changes from a decrement of approximately 3% for infinite crack spacing to an increment of approximately 8% for crack spacing equal to the crack length $c_0/L = d/L = 10$.

The increment in apparent toughness at the onset of crack growth for crack spacings d/L less than approximately 40 is in contrast to previous results on initial toughening where only a very slight increment in toughness appears for very long cracks and relatively high values of the transformation parameter ω.

R-curves for various initial crack lengths obtained by solving eqns (24) are shown in Fig. 14. The peaks in the apparent toughness induced by the transformation are the stronger the smaller the crack spacing. This is because of the well-known reduction in the stress intensity factor for an array of cracks compared to a single crack.

Strength curves for an array of surface cracks can be obtained from the following relation between the stress and stress intensity factors:

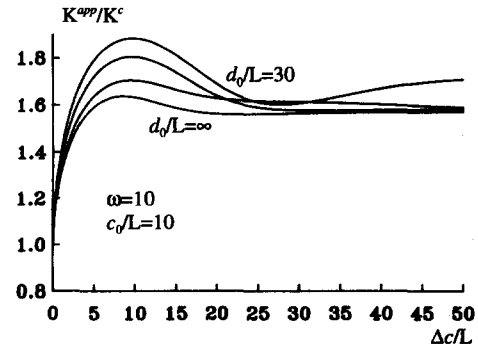

Fig. 14. R-curves for an array of surface cracks. d/L = 30, 50, 100, ∞.

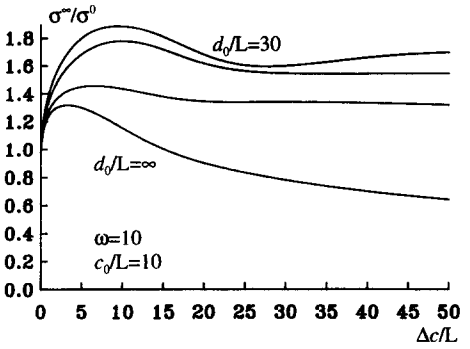

Fig. 15. Stress curves for an array of surface cracks. $d/L = 30, 50, 100, \infty$.

$$\frac{\sigma^{\infty}}{\sigma^{0}} = \frac{K^{\text{app}}}{K^{c}} \frac{B_0}{B} \sqrt{\frac{c_0}{c_0 + \Delta c}}, \tag{26}$$

where the effect of crack growth itself on strengthening has been incorporated. The normalising stress is the stress needed to initiate crack growth in the absence of transformation. B_0 is the geometrical amplification factor for the stress intensity factor pertaining to the initial crack configuration (Murakami, 1987). B is the corresponding geometrical factor pertaining to the changing geometry as the cracks are allowed to grow which is thus a function of the crack growth.

Stress curves corresponding to the R-curves are depicted in Fig. 15. The R-curve effect induces peaks in the stress curves which determine the ultimate strength of these ceramics. The presence of multiple surface cracks is therefore beneficial as compared with a single crack. In the limit when the steady-state conditions prevail the stress needed to give quasi-static crack growth becomes constant except for single surface cracks.

5. CONCLUDING REMARKS

The model presented for interacting surface cracks is expected to be well suited also for analysing situations where surface damage is expected to be an important factor. Before applying such an analysis however it is necessary to consider the stability of the cracks in the actual surface. This is not attempted in the present paper. However, the R-curve behaviour induced by transformation toughening should ensure a certain degree of stability in the crack growth. In the absence of transformation small variations in the lengths of cracks in the array in ideally brittle materials will cause only the longest crack to grow. In the presence of transformation however the R-curve behaviour counteracts this tendency, and crack growth can be expected from a large number of surface cracks before failure eventually is caused by the growth of the longest crack. Another important factor to be considered is crack path stability. Small variations in crack lengths or crack distances will cause the crack paths to depart from the straightness implied in the present model.

REFERENCES

Amazigo, J. C. and Budiansky, B. (1988). Steady-state crack growth in supercritically transforming materials. *Int. J. Solids Structures* **24**, 751–756.

Andreasen, J. H. (1990). Theoretical R-curves for internal cracks in transformation toughened materials. *Proc. 11 Risø Int. Symp. on Metallurgy and Materials Science* (Edited by J. J. Bentzen, J. B. Bilde-Sørensen, N. Christiansen, A. Horsewell and B. Ralph), pp. 161–166.

Andreasen, J. H. and Karihaloo, B. L. (1992). Mean stress criterion and internal cracks in transformation toughened ceramics. *Scripta Metall. et Mater.* **28**, 465–469.

Budiansky, B., Hutchinson, J. W. and Lambropoulos, J. C. (1983). Continuum theory of dilatant transformation toughening in ceramics. *Int. J. Solids Structures* **19**, 337–355.

Huang, X., Fraser, W. B. and Karihaloo, B. L. (1993). Contribution of first-order moduli differences to dilatant transformation toughening. *Int. J. Solids Structures* **30**, 151–160.

Karihaloo, B. L. (1991). Contribution of $t \rightarrow m$ phase transformation to the toughening of ZTA. *J. Am. Ceram. Soc.* **74**, 1703–1706.

Keer, L. M., Nemat-Nasser, S. and Oranratnachai, A. (1979). Unstable growth of thermally induced interacting cracks in brittle solids: further results. *Int. J. Solids Structures* **15,** 111–126.

McMeeking, R. M. and Evans, A. G. (1982). Mechanics of transformation toughening in brittle materials. *J. Am. Ceram. Soc.* **65,** 242–246.

Murakami, Y. (1987). *Stress Intensity Factor Handbook*. Pergamon Press, Oxford.

Nemat-Nasser, S., Keer, L. M. and Parihar, K. S. (1978). Unstable growth of thermally induced interacting cracks in brittle solids. *Int. J. Solids Structures* **14,** 409–430.

Nemat-Nasser, S., Sumi, Y. and Keer, L. M. (1980). Unstable growth of tension cracks in brittle solids: stable and unstable bifurcations, snap-through, and imperfection sensitivity. *Int. J. Solids Structures* **16,** 1017–1035.

Rose, L. R. F. (1987). The mechanics of transformation toughening. *Proc. R. Soc. Lond.* **A412,** 169–197.

Stump, D. M. (1992). Edge-crack resistance curves in supercritical ceramics. *J. Am. Ceram. Soc.* **75,** 889–895.

Stump, D. M. and Budiansky, B. (1989a). Crack-growth resistance in transformation toughened ceramics. *Int. J. Solids Structures* **25,** 635–646.

Stump, D. M. and Budiansky, B. (1989b). Finite cracks in transformation toughened ceramics. *Acta Metall.* **37,** 3297–3304.

APPENDIX

The weight functions for an array of surface cracks are obtained by summing the weight functions (9), (10), (14) and (15) for single surface cracks:

$$\begin{aligned} G^D(\underline{z}, \underline{z}_0) &= \sum_{k=-\infty}^{\infty} g^D(\underline{z}, x_0+kd, y_0) \\ G^T(\underline{z}, \underline{z}_0) &= \sum_{k=-\infty}^{\infty} g^T(\underline{z}, x_0+kd, y_0) \\ H^D(\underline{z}, \underline{z}_0) &= \sum_{k=-\infty}^{\infty} h^D(\underline{z}, x_0+kd, y_0) \\ H^T(\underline{z}, \underline{z}_0) &= \sum_{k=-\infty}^{\infty} h^T(\underline{z}, x_0+kd, y_0). \end{aligned} \tag{A1}$$

In order to obtain expressions for the weight functions for an array of parallel surface cracks it is expedient to rewrite the weight functions for a single surface crack as:

$$\begin{aligned} g^D(\underline{z}, kd, y_0) &= \left[2+(y+3y_0)\frac{\partial}{\partial y}+2yy_0\frac{\partial^2}{\partial y^2}\right]\frac{y+y_0}{(y+y_0)^2+(kd)^2}-\left[2+(y-y_0)\frac{\partial}{\partial y}\right]\frac{y-y_0}{(y-y_0)^2+(kd)^2} \\ g^T(\underline{z}, x_0+kd, y_0) &= \left[3+2y\frac{\partial}{\partial y}\right]\frac{y+y_0}{(y+y_0)^2+(x_0+kd)^2}-\frac{y-y_0}{(y-y_0)^2+(x_0+kd)^2} \\ h^D(\underline{z}, kd, y_0) &= \left[2+4y_0\frac{\partial}{\partial y}\right]\frac{y+y_0}{(y+y_0)^2+(x+kd)^2}-2\frac{y-y_0}{(y-y_0)^2+(x_0+kd)^2} \\ h^T(\underline{z}, x_0+kd, y_0) &= 4\frac{y+y_0}{(y+y_0)^2+(x-x_0+kd)^2}. \end{aligned} \tag{A2}$$

It is assumed in (A2) that one crack is located at $x = 0$. As the functions G^D and G^T enter the equation expressing the traction free condition across each crack in the array, the variable z is on the crack. The functions H^D and H^T on the other hand enter the equation that determines the boundary of the transformation zone of each crack, so the variable z is on this zone boundary. z_0 is a variable of integration. For G^D and H^D, z_0 is on the crack line, and for G^T and H^T, it is on the transformation zone boundary.

By using the following standard summation formulas:

$$\begin{aligned} \sum_{k=-\infty}^{\infty}\frac{\eta}{\eta^2+(b+kd)^2} &= \frac{\pi}{d}\frac{\sinh(2\pi\eta/d)}{\cosh(2\pi\eta/d)-\cos(2\pi b/d)} \\ \sum_{k=-\infty}^{\infty}\frac{\eta}{\eta^2+(kd)^2} &= \frac{\pi}{d}\coth(\pi\eta/d), \end{aligned} \tag{A3}$$

(A1) and (A2) give:

$$G^D(\underline{z}, \underline{z}_0) = \frac{\pi}{d}\left\{2\coth(\pi(y+y_0)/d)-\left(\frac{\pi}{d}\right)\frac{(y+3y_0)}{\sinh^2(\pi(y+y_0)/d)}+4\left(\frac{\pi}{d}\right)^2 yy_0\frac{\coth(\pi(y-y_0)/d)}{\sinh^2(\pi(y+y_0)/d)}\right.$$
$$\left.-2\coth(\pi(y-y_0)/d)+\left(\frac{\pi}{d}\right)\frac{(y-y_0)}{\sinh^2(\pi(y-y_0)/d)}\right\}$$

$$G^T(\underline{z}, \underline{z}_0) = \frac{\pi}{d}\left\{\frac{3\sinh(2\pi(y+y_0)/d)}{\cosh(2\pi(y+y_0)/d)-\cos(2\pi x_0/d)} + \frac{4\pi}{d}y\frac{1-\cosh(2\pi(y+y_0)/d)\cos(2\pi x_0/d)}{[\cosh(2\pi(y+y_0)/d)-\cos(2\pi x_0/d)]^2}\right.$$

$$\left. - \frac{\sinh(2\pi(y-y_0)/d)}{\cosh(2\pi(y-y_0)/d)-\cos(2\pi x_0/d)}\right\}$$

$$H^D(\underline{z}, \underline{z}_0) = \frac{\pi}{d}\left\{\frac{2\sinh(2\pi(y+y_0)/d)}{\cosh(2\pi(y+y_0)/d)-\cos(2\pi x/d)} + \frac{8\pi}{d}y\frac{1-\cosh(2\pi(y+y_0)/d)\cos(2\pi x/d)}{[\cosh(2\pi(y+y_0)/d)-\cos(2\pi x/d)]^2}\right.$$

$$\left. - \frac{2\sinh(2\pi(y-y_0)/d)}{\cosh(2\pi(y-y_0)/d)-\cos(2\pi x/d)}\right\}$$

$$H^T(\underline{z}, \underline{z}_0) = \frac{4\pi}{d}\left\{\frac{\sinh(2\pi(y+y_0)/d)}{\cosh(2\pi(y+y_0)/d)-\cos(2\pi(x-x_0)/d)}\right\}. \tag{A4}$$

The weight function $G^D(y, y_0)$ coincides with that of Nemat-Nasser *et al.* (1978).